# Comparison of $^{13}C(p,\pi^-)^{14}O^*$ and $^{13}C(p,\pi^+)^{14}C^*$ reactions in the region of the $\Delta_{1232}$ resonance

G. M. Huber and G. J. Lolos
*Department of Physics and Astronomy, University of Regina, Regina, Saskatchewan, Canada S4S 0A2*

R. D. Bent
*Indiana University Cyclotron Facility, Bloomington, Indiana 47405*

K. H. Hicks, P. L. Walden, and S. Yen
*TRIUMF, Vancouver, British Columbia, Canada V6T 2A3*

X. Aslanoglou*
*Department of Physics, Florida State University, Tallahassee, Florida 32306*

E. G. Auld
*Department of Physics, University of British Columbia, Vancouver, British Columbia, Canada V6T 2A6*

W. R. Falk
*Department of Physics, University of Manitoba, Winnipeg, Manitoba, Canada R3T 2N2*
(Received 1 July 1987)

The energy dependence of the $(p,\pi^-)$ and $(p,\pi^+)$ reactions on $^{13}C$ leading to isobaric analog states of $^{14}O$ and $^{14}C$ has been measured at a fixed four-momentum transfer at proton lab energies of 250, 354, and 489 MeV. Unlike the $(p,\pi^+)$ reactions, which show an enhancement of the differential cross section near the invariant mass of the $\Delta_{1232}$ similar to that observed for the $pp\rightarrow d\pi^+$ reaction at an equivalent center of mass energy and momentum transfer, the differential cross section of the $(p,\pi^-)$ reactions decrease with increasing energy through this region. This difference is consistent with an interpretation of the $(p,\pi^-)$ reaction mechanism as a $NN\rightarrow NN\pi^-$ process in which nonresonant amplitudes are dominant in this region.

## INTRODUCTION

From the beginning of its investigation, the $(p,\pi^-)$ reaction has been somewhat of a puzzle. Because of its small cross section and nearly featureless angular distribution, the $(p,\pi^-)$ reaction did not originally arouse the interest of early experiments, who preferred to study the more pronounced features of $(p,\pi^+)$ distributions.[1-4] The $(p,\pi^-)$ reaction was also neglected in the early formulation of $(p,\pi)$ theory. It cannot be directly accessed by a single-particle stripping mechanism, and although the featureless angular distribution is taken to be evidence of a multistep process involving many nucleons, only recently has work been done on two nucleon model calculations for $(p,\pi^-)$ reactions.[5-7]

Recently, interest in $(p,\pi^-)$ reactions was heightened by the results of a systematic study that revealed an unexpectedly strong selectivity of the reaction for the population of a closely spaced cluster of high-spin two-particle one-hole (2p-1h) final states.[8] This discovery was subsequently explained within the context of a $NN\rightarrow NN\pi^-$ reaction model.[9] Further signatures of a $NN\rightarrow NN\pi^-$ process in the $(p,\pi^-)$ reaction mechanism were also seen at the Indiana University Cyclotron Facility (IUCF), such as the behavior of the analyzing powers of the $^{12,13,14}C(p,\pi^-)$ $^{13,14,15}O_{g.s.}$ transitions[10] (g.s. is ground state) and the stable analyzing power shape for $(p,\pi^-)$ reactions to high-spin stretched 2p-1h states on a variety of nuclear targets.[11] Additional $NN\rightarrow NN\pi^-$ signatures in $(p,\pi^-)$ reactions are contained in a recent paper by Throwe *et al.*[12]

The role of $NN\rightarrow NN\pi^+$ processes in $(p,\pi^+)$ reactions is less well known. This is partly because single nucleon stripping mechanism processes can also contribute to $(p,\pi^+)$ reactions. Nevertheless, there is some evidence[13] that $\Delta_{1232}$ resonant $NN\rightarrow NN\pi^+$ processes do play a significant role in $(p,\pi^+)$ reactions. In particular, previous investigations[13,14] of the $(p,\pi^+)$ reaction indicate that the differential cross section is enhanced in the region of the $\Delta_{1232}$ resonance, similar to that shown by the elementary $pp\rightarrow d\pi^+$ reaction. This can be interpreted as a signature of $NN\rightarrow NN\pi^+$ processes occurring within the nuclear environment. Furthermore, analyzing powers of the $(p,\pi^+)$ reaction to the continuum in the kinematical region close to the exclusive reaction limit show great similarities to the $pp\rightarrow d\pi^+$ reaction.[15] For the $(p,\pi^-)$ reaction, differential cross sections have only been obtained at energies far above, or well below the $\Delta_{1232}$ region, so it has not been proven whether $(p,\pi^+)$ and $(p,\pi^-)$ reactions exhibit a similar energy dependence. It would thus be desirable to have complete measurements across the $\Delta_{1232}$ region for both $(p,\pi^+)$ and

 

$(p,\pi^-)$ reactions to investigate such questions relating to the dynamical behavior of the two processes.

To elucidate the role of the $\Delta_{1232}$ isobar in the $(p,\pi^-)$ reaction, we have performed an experiment at TRIUMF with an unpolarized beam to compare the energy dependencies of the $(p,\pi^-)$ and $(p,\pi^+)$ reactions on $^{13}C$ leading to mirror states of $^{14}O$ and $^{14}C$. Beam energies of 250, 354, and 489 MeV were chosen because a simple calculation shows that the peak of the $\Delta_{1232}$ excitation would occur at a beam energy of 320 MeV if the beam proton and $^{13}C$ target combined to form a mass 14 nucleus in which one nucleon is excited to a mass of 1232 MeV. Thus, if the $(p,\pi^-)$ reaction is dominated by the $NN \rightarrow \Delta N \rightarrow NN\pi^-$ process, the effect of intermediate $\Delta_{1232}$ formation should be pronounced in this energy range. By choosing mirror final states, effects due to differences in nuclear structure are minimized, and any differences in the energy behavior of the $(p,\pi^-)$ and $(p,\pi^+)$ differential cross sections at the same four momentum transfer should primarily reflect differences in reaction mechanism behavior rather than nuclear structure. We note, however, that this comparison is only valid to first order since the $(p,\pi^+)$ and $(p,\pi^-)$ reactions are not mirrors of each other and, therefore, they can sample different isospin components of a given mirror pair of final states.

The merit of measuring the energy dependence of the cross section at a constant $t$ (square of the four-momentum transfer) is that nuclear structure effects are fixed[14] to first order and, hence, the energy behavior of the cross section reflects the energy behavior of the reaction mechanism. This statement can be simply illustrated by using a transformation described in Ref. 15 where a real $pp \rightarrow d\pi^+$ process is forced to reproduce the $(p,\pi^+)$ kinematics. At $t = 0.5$ GeV$^2/c^2$ the required nuclear proton momentum for this transformation is a constant 238 MeV/$c$ to within about 2 MeV/$c$ for beam energies from 200 to 800 MeV. Not only is this a reasonable value of nuclear momentum for this nucleus, but it is nearly independent upon incident proton energy. Hence the nuclear medium effect on the cross section should be relatively constant. The transformation of Ref. 15 is a plane wave calculation and one would expect that at resonant energies distortions will play a major role, possibly modifying our statements. However, for both the $(p,\pi^+)$ and $(p,\pi^-)$ reactions on $^{13}C$ the incoming channel distortions are common and the distortions in the outgoing channel between $\pi^+$-$^{14}C$ and $\pi^-$-$^{14}O$ are assumed to have similar dynamic behaviors. Thus, although distortions as final state interactions are energy dependent and can affect the momentum transfer, the comparisons of the $(p,\pi^+)$ and $(p,\pi^-)$ reactions at the same energies should be almost insensitive to the effects of the final state interactions and the fixed $t$ values should still be the best one can do in minimizing the nondynamical variables. A four-momentum transfer squared of $t = 0.5$ GeV$^2/c^2$ was chosen for this study because it is nearly the largest momentum transfer accessed at 180 MeV, and is approximately the smallest momentum transfer accessed at 489 MeV. Thus, it is the only four-momentum transfer for which a comparison can be made from close to pion production threshold to well above the $\Delta_{1232}$ invariant mass.

## EXPERIMENT

Data were taken with the Medium Resolution Spectrometer (MRS) at TRIUMF during two runs. The proton beam was incident on a research grade $^{13}C$ target of $94 \pm 1$ mg/cm$^2$ thickness. The target angle with respect to the beam was chosen at each spectrometer angle setting so that the energy loss of the proton beam in the target would be approximately equal to the energy loss of the detected pions in order to optimize the energy resolution of the MRS. An error of 2° in the target angle calibration corresponds to a relative uncertainty in the target thickness of approximately 4%.

Beam intensity was monitored continuously by an in-beam polarimeter and by a secondary emission monitor (SEM), both of which were previously calibrated against a Faraday cup. The polarimeter consisted of a $CH_2$ target of 1.383 mg/cm$^2$ thickness and two pairs of counter telescopes, each in coincidence with a recoil counter, that detect elastic proton-proton scattering events. Agreement between the two monitors for total charge on target was usually within 4%, however, SEM was used for the beam normalization since the thin polarimeter target has been known to wrinkle after an extended time period in the beam. The location and size of the beam spot (typically 2.5 cm $\times$ 0.5 cm $XY$ in dispersed mode) was visually monitored periodically with a scintillator located at the target position.

Because the CAMAC scalers of the MRS are not inhibited when the data acquisition system is busy, all scalers must be corrected by the live time of the instrument. This live time was measured by two independent means. It can be simply measured by taking the ratio of the number of busy latches that the data acquisition electronics generates divided by the number of event triggers. The MRS electronics also contains provision for generating pseudoevents electronically. The ratio of the number of these pseudoevents actually seen by the acquisition system, divided by the number of pseudoevents generated, gives a second determination of the live time. In most cases the two different methods were within 2% of each other; during the $(p,\pi^-)$ runs the live time was approximately 98%.

The effective solid angle of the MRS spectrometer was determined relative to the very accurately known cross section of the $pp \rightarrow d\pi^+$ reaction[16] at a proton energy of 500 MeV, an energy which yields pions of momentum similar to those from the reactions of interest. The effective solid angle of the spectrometer was determined by this method to be 2.1 msr, with a standard deviation of 0.1 msr between independent calibrations. This solid angle was found to be independent of beam spot size and pion energy within this uncertainty.

The spectrometer detection system consisted of a multiwire drift chamber located in front of the spectrometer's entrance quadrupole, and two vertical drift chambers followed by two levels of plastic scintilla-

tors located near the focal plane of the spectrometer. The two levels of scintillators, along with one plane of the front end chamber, and one plane of the first of the two vertical drift chambers, provided the event definition. The product of the efficiency of all three chambers was typically 75% for $(p,\pi^+)$ runs, and 50% for $(p,\pi^-)$ runs. This decrease in efficiency was shared equally between all three chambers, and was primarily due to increased beam current during the $(p,\pi^-)$ runs in order to reduce the running time, resulting in increased double hits from the background.

Because $(p,\pi^-)$ reactions have very low cross sections, background problems warrant careful consideration. The use of a front end wire chamber provides a high degree of redundancy as it allows a complete ray trace through the spectrometer back to the target, a distance of about 11 m. Therefore, all background sources not originating from the illuminated target spot could be eliminated. Most of the muons resulting from pion decay within the spectrometer were eliminated via the beam spot and solid angle cuts; net events observed were then corrected for pion decay within the spectrometer. This pion survival fraction was approximately 35% at 250 MeV, 50% at 354 meV, and 65% at 489 MeV. In addition, when using a magnetic spectrometer the proton background problem associated with $(p,\pi^+)$ experiments is reduced in $(p,\pi^-)$ experiments due to the negative charge of the pions; this, coupled with the redundancy of the cuts applied in the off-line event-by-event analysis made it possible to observe states with differential cross sections as low as 0.5 nb/sr.

The energy resolution obtained was 180 keV at 354 MeV in the first data taking run and 300 keV in the second run. The poorer energy resolution in the second run was due to a larger than usual energy spread of the incident proton beam from the TRIUMF cyclotron (0.35% $\Delta p/p$ instead of 0.2% $\Delta p/p$). Data from the first and second runs cannot be directly compared because different angles were studied in each run; however, where the two data sets overlapped there was agreement within the statistical uncertainties. The poorer energy resolution of the second run did not affect the minimum observable $(p,\pi^-)$ cross section.

## RESULTS

Off-line analyzed pion spectra from the first run (after solid angle, energy loss, time of flight, and target illumination cuts) are shown in Figs. 1 and 2. Both spectra shown in Fig. 1 are dominated by a $3^-$ state near 6 MeV excitation, which has predominantly a two-particle one-hole configuration (2p-1h) with respect to the $^{13}C_{g.s.}$. Note that at 250 MeV the momentum acceptance of the spectrometer was not large enough to allow data from states ranging from the $^{14}C_{g.s.}$ to $^{14}C^*_{23.2}$ to be collected simultaneously. At this energy, data were obtained with two magnetic field settings of the spectrometer; only data from the highest field setting are shown in Fig. 1.

At 354 MeV, the acceptance of the spectrometer was large enough to view the entire energy range, as shown in Fig. 2. The high spin 11.67 and 14.87 MeV states

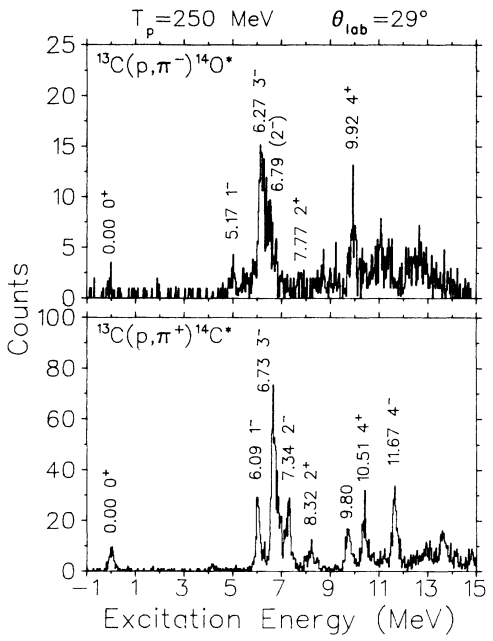


FIG. 1. 250 MeV focal plane spectra from the first run of the experiment taken at a four-momentum transfer squared of $t=0.57$ GeV$^2/c^2$.

dominate the $(p,\pi^+)$ spectrum shown in Fig. 2, as one would expect considering the high momentum transfer of this reaction. In addition, the 23.2 MeV state of $^{14}C$, which has been previously observed[15] to have an unusual zero analyzing power, is clearly visible. The absence of a strongly populated mirror state in $^{14}O$ near 23 MeV excitation at 354 and 489 MeV indicates, by isospin arguments, that this is not a $T=2$ state, and confirms arguments presented in Ref. 15. The 13.50 and 14.05 MeV states of $^{14}C^*$ shown in Fig. 2 are reasonably populated but are not listed in the nuclear level tables of

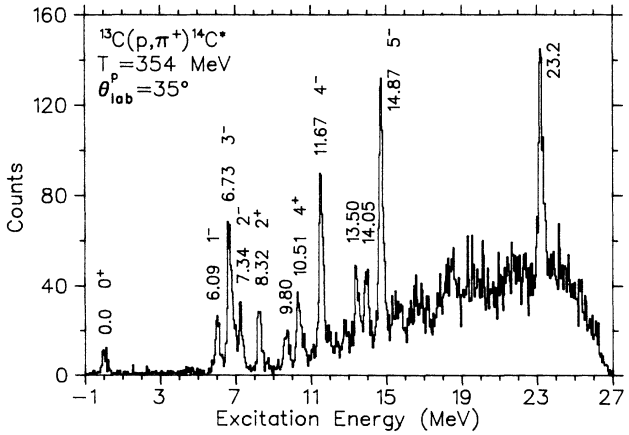


FIG. 2. 354 MeV $(p,\pi^+)$ focal plane spectrum from the first run of the experiment taken at a four-momentum transfer squared of $t=0.47$ GeV$^2/c^2$. The spin assignment of the 11.67 and 14.87 MeV states is taken from Ref. 15 instead of Ref. 17.

TABLE I. A list of values of differential cross sections for selected final states of the $^{13}C(p,\pi^-)^{14}O^*$ reaction. All quantities shown are in the center of mass frame; angles are in degrees and $d\sigma/d\Omega$ are in nb/sr. The numbers in parentheses reflect statistical uncertainties only. The systematic error in the overall normalization has been estimated at 8%, and the relative uncertainty has been estimated at 10%.

| | | $^{13}C(p,\pi^-)$ | | |
|---|---|---|---|---|
| $\theta_{c.m.}$ | $^{14}O_{g.s.}$ | $^{14}O^*_{5.17}$ | $^{14}O^*_{6.27,6.79}$ | $^{14}O^*_{9.92}$ |
| | | $T_p=250$ MeV | | |
| 31 | 2.3(0.7) | 5.8(1.2) | 68.2(4.0) | 17.4(2.1) |
| 52 | 1.6(0.4) | 3.3(0.6) | 44.5(0.2) | 8.2(1.0) |
| | | $T_p=354$ MeV | | |
| 32 | 1.6(0.4) | | 19.8(1.5) | |
| | | $T_p=489$ MeV | | |
| 21 | 0.6(0.3) | | 4.7(0.9) | |

Ajzenberg-Selove.[17] These states are also visible in the pion spectrum obtained[15] at 200 MeV.

Because of the close spacing of the populated levels near 6 MeV, a peak fitting routine[18] was used to deconvolute these states. This procedure was a necessity for the poorer resolution spectra obtained from the second run, but was also performed on the spectra from the first run in order to be consistent. For the states shown in Fig. 1, the peak fitting routine was used to deconvolute the 6.09 and 7.34 MeV states from the 6.73 MeV peak of $^{14}C$. It should be noted that the 6.73 MeV state is close in energy to a cluster of other states (6.59, 6.90, and 7.01 MeV). The deconvolution routine shows that these states are most probably weak in comparison to the 6.73 MeV state, so no attempt was made to subtract their strengths from the 6.73, $3^-$ peak. For the $(p,\pi^-)$ spectra, no attempt was made to deconvolute the 6.79 MeV state of $^{14}O$ from the 6.27 MeV peak because of poor statistics. Differential cross sections for all states are listed in Tables I and II. Systematic and relative errors are summarized in Table III.

Plots of differential cross section versus center of mass energy at a constant four-momentum transfer are shown for the $^{13}C(p,\pi^-)^{14}O_{g.s.}$ and $^{13}C(p,\pi^+)^{14}C_{g.s.}$ reactions in Fig. 3, and for the $^{13}C(p,\pi^-)^{14}O^*_{6.27,6.79}$, $^{13}C(p,\pi^+)^{14}C^*_{6.73}$ and $^{13}C(p,\pi^+)^{14}C^*_{23.2}$ reactions in Fig. 4. These figures plot data from this work, as well as other previously published data[8,10,15,19,20] using the relativistically invariant Mandelstam variables $s$ and $t$. The choice of $s$ and $t$ is dictated by the fact that the unpolarized scattering amplitude is only a function of $s$ and $t$, as far as the kinematic variables are concerned. The quantity $\sqrt{s}-m_{^{13}C}$ is a measure of the excitation energy available for one nucleon. The cross sections shown in Figs. 3 and 4 at $t=0.50$ GeV$^2/c^2$ were obtained by interpolation using fits to the data. For the data below $T_p=250$ MeV,[8,10,15,19,20] Legendre polynomial fits to the angular distribution results were used. For $T_p=250$ MeV and above, which are the data from this work, an exponential was fitted to the cross section at the two angles mea-

TABLE II. A list of values of differential cross sections for selected final states of the $^{13}C(p,\pi^+)^{14}C^*$ reaction.

| | | $^{13}C(p,\pi^+)$ | | | | | | | | | | |
|---|---|---|---|---|---|---|---|---|---|---|---|---|
| $\theta_{c.m.}$ | $^{14}C_{g.s.}$ | $^{14}C^*_{6.09}$ | $^{14}C^*_{6.73}$ | $^{14}C^*_{7.34}$ | $^{14}C^*_{8.32}$ | $^{14}C^*_{9.80}$ | $^{14}C^*_{10.51}$ | $^{14}C^*_{11.67}$ | $^{14}C^*_{12.86}$ | $^{14}C^*_{13.5}$ | $^{14}C^*_{14.05}$ | $^{14}C^*_{14.87}$ | $^{14}C^*_{15.44}$ | $^{14}C^*_{23.2}$ |
| | | | | $T_p=250$ MeV | | | | | | | $T_p=250$ MeV | | | |
| 31 | 127(14) | 373(25) | 1180(44) | 356(24) | 149(16) | 235(20) | 344(24) | 520(32) | | | | | | |
| 52 | 27.6(3.3) | 122(7) | 341(12) | 80.9(5.8) | 54.6(4.8) | 79.6(5.9) | 88.7(5.6) | 195(8) | 65.4(4.5) | 58.3(4.3) | 48.2(3.9) | 214(8) | | 290(12) |
| | | | | $T_p=354$ MeV | | | | | | | $T_p=354$ MeV | | | |
| 30 | 57.9(6.4) | 117(9) | 783(23) | 188(11) | 169(11) | 112(9) | 235(13) | 530(19) | 78.5(7.2) | 200(12) | 224(12) | 647(21) | 110(9) | 597(34) |
| 37 | 42.3(5.1) | 88.0(7.1) | 253(12) | 80.4(6.8) | 88.1(7.1) | 49.9(5.5) | 112(8.1) | 279(13) | 36.8(0.5) | 115(8) | 108(8) | 397(15) | | 500(20) |
| | | | | $T_p=489$ MeV | | | | | | | $T_p=489$ MeV | | | |
| 21 | 26.2(5.0) | 60.2(7.2) | 279(16) | 62.4(7.5) | 73.0(8.0) | 27.8(5.0) | 70.0(7.7) | 231(14) | 18.7(0.4) | 66.7(8.0) | 28.9(5.2) | 292(16) | 18.0(4.0) | 271(16) |
| 32 | 8.1(1.6) | 28.5(2.9) | 75.7(4.7) | 26.5(2.7) | 18.4(2.4) | 5.7(1.3) | 8.8(1.6) | 45.0(3.7) | | 11.2(1.8) | 13.3(2.0) | 89.6(5.1) | 21.3(2.6) | 53.7(4.0) |

sured. For the $T_p = 354$ and 489 MeV, $(p,\pi^-)$ results, where the cross section was measured at only one angle, the relative exponential fit to the 250 MeV data was used. Since the data in this experiment were measured close to $t = 0.5$ GeV$^2/c^2$, the error involved in this interpolation is minimal.

Plotting the differential cross section at a constant four-momentum transfer permits, as discussed previously, the first order separation of the reaction mechanism from the nuclear structure effects.[14] Any differences in the energy behavior of the $(p,\pi^-)$ and $(p,\pi^+)$ differential cross sections can then be attributed mainly to the reaction mechanism. Both Figs. 3 and 4 show that at $t = 0.50$ GeV$^2/c^2$ the $(p,\pi^+)$ reactions have an enhancement in the differential cross section near the invariant mass of the $\Delta_{1232}$ ($\sqrt{s} - m_{^{13}C} = 1.232$ GeV). This enhancement has been noted previously for the $^2$H, $^3$He, $^9$Be, $^{10}$B, $^{12}C(p,\pi^+)$ reactions near this momentum transfer.[2,13,14,21] For comparison, the differential cross section of the $pp \rightarrow d\pi^+$ reaction, in which the $\Delta_{1232}$ resonance is known to play a dominant role, and referred to the nucleon-nucleus frame using the transformation of Ref. 15, is plotted at a constant momentum transfer of $t = 0.50$ GeV$^2/c^2$ at the bottom of Fig. 3. It is easily seen that the energy dependence of the $pp \rightarrow d\pi^+$ and $(p,\pi^+)$ reactions is strikingly similar. The addition of $pp \rightarrow pn\pi^+$ contributions to the $pp \rightarrow d\pi^+$ plot would enhance the high energy tail and cause it to more closely resemble the $^{13}C(p,\pi^+)$ energy dependence. This energy dependence is common to other $(p,\pi^+)$ reactions at four-momentum transfers greater than $t = 0.45$ GeV$^2/c^2$.[13]

In contrast, the differential cross sections of both $(p,\pi^-)$ reactions in Figs. 3 and 4 show no enhancement near the invariant mass of the $\Delta_{1232}$. These are the first measurements of the energy dependence of the $(p,\pi^-)$ reaction in this dynamical region. The combination of the

TABLE III. Sources of error, and their assigned values for this experiment.

| | |
|---|---|
| **Systematic errors** | |
| Solid angle | ±6% |
| Pion survival factor | 5% |
| Uncertainty in $pp \rightarrow d\pi^+$ normalization | 2% |
| Target thickness | 1% |
| Total systematic error | ±8% |
| **Relative errors** | |
| Cut efficiencies and background subtraction | ±8% |
| Target angle | 4% |
| Acquisition system live time | 3% |
| Integrated beam current | 2% |
| Wire chamber efficiency | 2% |
| Focal plane relative efficiency | 2% |
| Total relative error | ±10% |

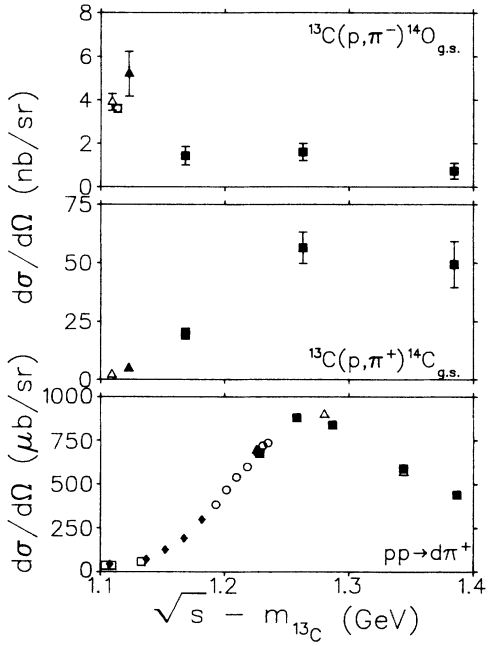


FIG. 3. Differential cross section versus center-of-mass energy ($\sqrt{s} - m_{^{13}C}$) at a constant four-momentum transfer ($t$) of 0.50 GeV$^2/c^2$ for the ground state transitions. Plotting symbols indicate the source of data as follows: △ (Ref. 19) 185 MeV; ○ (Ref. 10) 190 MeV; ▲ (Ref. 20) 200 MeV; ■ (this work) 250, 354, 489 MeV. Also shown are the differential cross sections for the $pp \rightarrow d\pi^+$ reaction with modifications as described in the text. Plotting symbols indicate the source of data as follows: ♦ (Ref. 16); ■ (Ref. 25); □ (Ref. 26); △ (Ref. 27); ○ (Ref. 28). The data from Refs. 25-27 were extracted from Legendre polynomial fits contained in Ref. 29. The error bars reflect statistical uncertainties only.

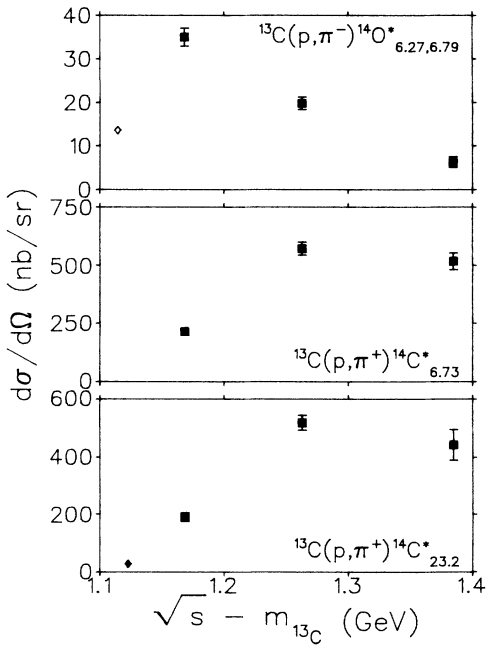


FIG. 4. Same as in Fig. 3 except for high-spin final states. Plotting symbols are the same as in Fig. 3 except ◇ (Ref. 8) 191 MeV; ♦ (Ref. 15) 200 MeV.

small $(p,\pi^-)$ cross section and the 2.1 msr spectrometer solid angle made it impractical to obtain a distribution of $(p,\pi^-)$ differential cross sections over a large angular range (corresponding to a large range of $t$ values). However, it has been shown in Ref. 13 for the $^{12}C(p,\pi^+)^{13}C^*$ reaction that the energy dependence of the differential cross section at constant momentum transfer is independent of the $t$ value chosen within the range of $0.7 > t > 0.45$ GeV$^2/c^2$. No angular distribution results exist for the $^{13}C(p,\pi^+)^{14}C^*$ reaction at higher energies. Nevertheless, the similarity of the energy dependence of this reaction, as shown in Figs. 3 and 4, to those shown in Refs. 13 and 14 suggests that this feature is a general characteristic of $(p,\pi^+)$ reactions in this range of four-momentum transfers. Thus, we expect that the energy dependencies shown for the $(p,\pi^+)$ reaction are not very sensitive to the $t$ value chosen within this range. Although angular distributions for $(p,\pi^-)$ reactions are not available over a similarly large energy range, recently published $(p,\pi^-)$ angular distributions[12,22,23,24] which include nuclei from $^7$Li to $^{48}$Ca do not exhibit dips and wiggles. This leads us to expect that the energy dependencies of $(p,\pi^-)$ reactions are similarly insensitive to the momentum transfer chosen within this range of $t$ values. Although the energy dependencies of the two $(p,\pi^-)$ reactions are somewhat different, the most important feature is the lack of an enhancement of the cross section in the $\Delta_{1232}$ region. This common feature of two transitions to two entirely different final states indicates that, in addition to any differences which nuclear structure may cause, there is a substantial dynamical difference between the $(p,\pi^-)$ and $(p,\pi^+)$ reactions. We note that the $(p,\pi^+)$ transitions to mirror final states exhibit a common energy dependence which is markedly different than that exhibited by either of the $(p,\pi^-)$ reactions.

As an added measure for comparison, the squares of the invariant matrix elements were extracted from the differential cross sections in order to remove any effects due to an increase in phase space as the energy increases. This extraction was done using the equation for $A(p,\pi)A+1$ reactions in general

$$|M|^2 = \frac{64\pi^2}{\hbar^2 c^2} s \left[\frac{k_p}{k_\pi}\right] \frac{(2J_A+1)(2S_p+1)}{(2J_{A+1}+1)(2S_\pi+1)} \left[\frac{d\sigma}{d\Omega}\right],$$

where $s$ is the Mandelstam variable previously described, and the other symbols are standard and referring to the center of mass frame. The results are plotted in Figs. 5 and 6. These plots clearly indicate again that there is a substantial difference between the $(p,\pi^-)$ and $(p,\pi^+)$ reaction mechanisms.

## DISCUSSION

The $NN \rightarrow NN\pi^-$ dominance of the $(p,\pi^-)$ reaction mechanism has been a widely accepted assumption.[12] The role of the $\Delta_{1232}$ resonance in the $(p,\pi^-)$ reaction, however, is currently an open question.[35,36] The striking differences between the $(p,\pi^+)$ and $(p,\pi^-)$ energy dependencies shown in Figs. 3–6 suggest that the role of the $\Delta_{1232}$ is distinctly different in the two reactions.

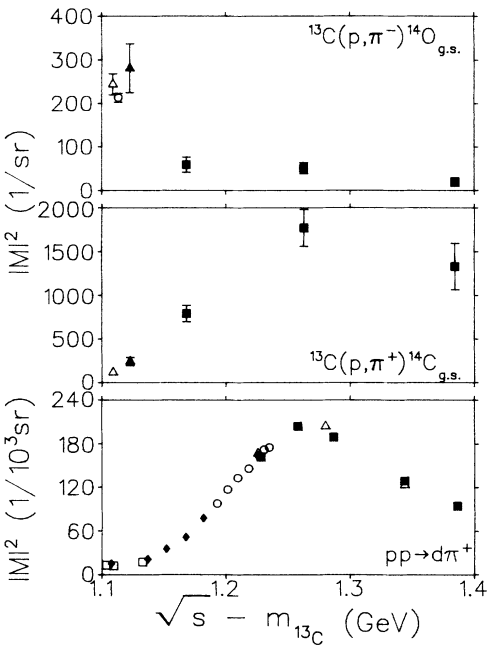


FIG. 5. Invariant matrix element (as explained in the text) plotted versus center-of-mass energy $\sqrt{s} - m_{^{13}C}$ at a constant four-momentum transfer ($t$) of 0.50 GeV$^2/c^2$ for the ground state transitions as well as the pp→dπ+ reaction. Plotting symbols are the same as in Fig. 3.

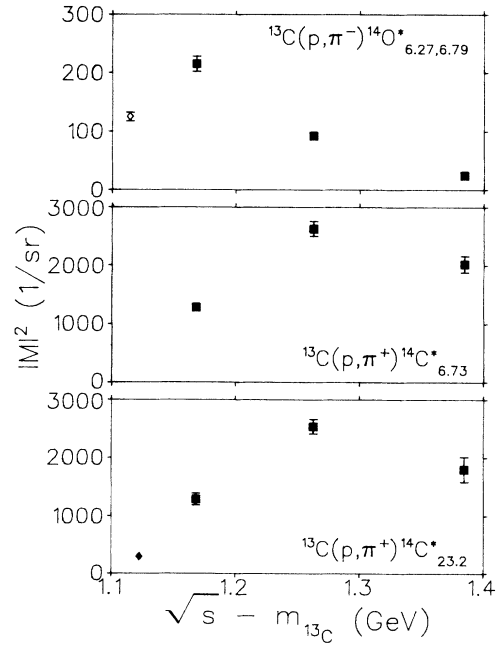


FIG. 6. Same as in Fig. 5 except for high-spin final states. Plotting symbols are as in Fig. 4. A final state spin of 3 was used in the matrix element calculation for all three of these plots.

It is well known[30–34] that the dominant amplitude for the $pp \rightarrow pn\pi^+$ reaction in the $\Delta_{1232}$ resonance region is $pp(^1D_2) \rightarrow \Delta N(^5S_2) \rightarrow pn(^3S_1) + P$-wave $\pi^+$. This amplitude is forbidden for the $pn \rightarrow pp\pi^-$ reaction by angular momentum and parity conservation and the Pauli principle. Allowed $\Delta_{1232}$ channels for $\pi^-$ production in a two-nucleon mechanism are $pn(^3P_0) \rightarrow \Delta N(^3P_0) \rightarrow pp(^1S_0) + S$-wave $\pi^-$ and $pn(^1D_2) \rightarrow \Delta N(^5S_2) \rightarrow pp(^3P_2) + S$-wave $\pi^-$ involving $P$ waves for either the intermediate $\Delta N$ or final NN state, as well as other channels involving still higher partial waves. These resonant amplitudes are much smaller than the one above that dominates the $pp \rightarrow pn\pi^+$ reaction,[34] and may be masked in the $(p,\pi^-)$ reaction by nonresonant amplitudes. A recent analysis of analyzing power data for $(p,\pi^-)$ reactions on nuclei[35] together with a phase shift analysis of differential cross sections for low-energy $\pi^-$ absorption by a $^1S_0$, $T=1$ proton pair in $^3$He (Ref. 36) suggests that the $pn \rightarrow pp\pi^-$ reaction at low energies may be dominated by the nonresonant $pn(^3D_1, T=0) \rightarrow pp(^1S_0)$ transition, which cannot access an intermediate $\Delta N(T=1,2)$ state. This may be the reason for the lack of an enhancement of the $(p,\pi^-)$ reaction near the invariant mass of the $\Delta_{1232}$. It should be noted that other considerations, such as the possible influence of higher energy $\pi$N resonances that only the $(p,\pi^-)$ reaction can access, or possible differences in $\pi^+$ and $\pi^-$ absorption by the nuclear medium, may further influence the energy dependence of the $(p,\pi^-)$ reaction.

Alternatively, the possibility exists that the $(p,\pi^-)$ reaction may be a two step process involving pion single charge exchange. In this case, recent results from pion-nucleus single charge exchange studies at the Los Alamos Meson Physics Facility (LAMPF) (Ref. 37) may have direct bearing on this discussion. This reference indicates that the $(\pi^+,\pi^0)$ reaction on a wide variety of nuclei exhibits the influence of the $\Delta_{1232}$ resonance by a suppression of the cross section in the $\Delta_{1232}$ region due to increased absorption of the outgoing pion in the nuclear medium. Detailed model calculations are needed to clarify the role of the $\Delta_{1232}$ in the $A(p,\pi^-)A+1$ reaction.

## SUMMARY AND CONCLUSIONS

The energy dependence of the $^{13}C(p,\pi^-)^{14}O^*$ and $^{13}C(p,\pi^+)^{14}C^*$ reactions leading to mirror final states has been measured in the region where $\Delta_{1232}$ resonance effects should be maximal. At the four-momentum transfer investigated, the excitation functions of the $(p,\pi^+)$ reactions show an enhancement near the invariant mass of the $\Delta_{1232}$ similar to that exhibited by the $pp \rightarrow d\pi^+$ reaction, which proceeds mainly through intermediate delta formation. The differential cross sections of the $(p,\pi^-)$ reactions, on the other hand, do not exhibit this enhancement. This lack of an enhancement at the invariant mass of the $\Delta_{1232}$ is also seen in the energy dependence of the invariant matrix element (Figs. 5 and 6), which does not include the gradual increase in phase space over the energy range. This difference is consistent with an interpretation of the $(p,\pi^-)$ reaction mechanism as a $NN \rightarrow NN\pi^-$ process in which intermediate $\Delta_{1232}$ formation is much less important in the $(p,\pi^-)$ reaction than in the $(p,\pi^+)$ reaction.

These results should spur additional development of current theoretical models. At present, existing Two Nucleon Model codes[5,38,39] include only rescattering via $\Delta_{1232}$ formation and neglect nonresonant contributions. Microscopic $\Delta$-hole calculations[40] including nonresonant terms have not yet been applied to $(p,\pi^-)$ reactions. Further experimental work is also necessary to clear up questions about the sensitivity of the energy dependence of the $(p,\pi^-)$ reaction to momentum transfer ($t$) and to nuclear structure effects.

## ACKNOWLEDGMENTS

The authors would like to thank D. Frekers, K. P. Jackson, and C. A. Miller for their assistance in this experiment, and also E. D. Cooper and M. Dillig for their valuable comments. This experiment was funded in part by grants from the Natural Sciences and Engineering Research Council of Canada (NSERC).

*Present address: Department of Physics and Astronomy, Ohio University, Athens, OH 45701.

[1] D. F. Measday and G. A. Miller, Annu. Rev. Nucl. Part. Sci. **29**, 121 (1979).

[2] B. Hoistad, in *Advanced Nuclear Physics,* edited by J. W. Negele and E. Vogt (Plenum, New York, 1979), Vol. 11, p. 135; B. Hoistad, in *Pion Production and Absorption in Nuclei—1981 (Indiana University Cyclotron Facility),* Proceedings of the Conference on Pion Production and Absorption in Nuclei, AIP Conf. Proc. No. 79, edited by Robert D. Bent (AIP, New York, 1982), p. 105.

[3] H. W. Fearing, in *Progress in Particle and Nuclear Physics,* edited by D. Wilkinson (Pergamon, New York, 1981), Vol. 7, p. 113.

[4] P. Couvert, in Proceedings of the Workshop on Studying Nuclei with Medium Energy Protons, Edmonton, 1983, TRIUMF Report TRI-83-3, 287, 1983 (unpublished).

[5] M. Dillig, J. S. Conte, and R. D. Bent, Indiana University Cyclotron Facility Sci. Tech. Report 25, 1985 (unpublished). P. W. F. Alons, R. D. Bent, J. S. Conte, and M. Dillig, Nucl. Phys. A (to be published).

[6] P. Couvert and M. Dillig, Phys. Rev. C **32**, 354 (1985).

[7] K. Kume, Proceedings of the Sixth International Symposium on Polarization Phenomenon in Nuclear Physics, Osaka, 1985 [J. Phys. Soc. Jpn. Suppl. **55**, 920 (1986)].

[8] S. E. Vigdor *et al.*, Nucl. Phys. **A396**, 61c (1983).

[9] B. A. Brown, O. Scholten, and H. Toki, Phys. Rev. Lett. **51**, 1952 (1983).

[10]W. W. Jacobs *et al.*, Phys. Rev. Lett. **49**, 855 (1982).
[11]H. Toki and K. I. Kubo, Phys. Rev. Lett. **54**, 1203 (1985).
[12]T. G. Throwe *et al.*, Phys. Rev. C **35**, 1083 (1987).
[13]G. M. Huber *et al.*, Phys. Rev. C **36**, 1058 (1987).
[14]P. Couvert and M. Dillig, Abstracts of the International Conference on High Energy Physics and Nuclear Structure, Versailles, 1981 (unpublished), p. 192.
[15]E. Korkmaz *et al.*, Phys. Rev. Lett. **58**, 104 (1987).
[16]G. L. Giles, Ph.D. thesis, University of British Columbia, 1985.
[17]F. Ajzenberg-Selove, Nucl. Phys. **A449**, 1 (1986).
[18]J. W. Rowson, Ph.D. thesis, University of Regina, 1978.
[19]S. Dahlgren, P. Grafstrom, B. Hoistad, and A. Asberg, Phys. Lett. **47B**, 439 (1973).
[20]B. Hoistad *et al.*, Phys. Lett. **94B**, 315 (1980).
[21]P. Couvert, in Proceedings of the Conference on the Intersections Between Particle and Nuclear Physics, Steamboat Springs, 1984, TRIUMF Report TRI-PP-84-46, 1984.
[22]Z. J. Cao *et al.*, Phys. Rev. C **35**, 825 (1987).
[23]B. Hoistad *et al.*, Phys. Lett. **177B**, 299 (1986).
[24]J. J. Kehayias *et al.*, Phys. Rev. C **33**, 1388 (1986).
[25]C. Richard-Serre *et al.*, Nucl. Phys. **B20**, 413 (1970).
[26]B. G. Ritchie *et al.*, Phys. Rev. C **24**, 552 (1981).
[27]J. Boswell *et al.*, Phys. Rev. C **25**, 2540 (1982).
[28]J. Hofteizer *et al.*, Nucl. Phys. **A402**, 429 (1983).
[29]G. Jones, in *Pion Production and Absorption in Nuclei—1981 (Indiana University Cyclotron Facility)*, Ref. 2, p. 15.
[30]A. W. Thomas and R. H. Landau, Phys. Rep. **58C**, 121 (1980).
[31]M. Betz, B. Blankleider, J. A. Niskanen, A. W. Thomas, in *Pion Production and Absorption in Nuclei—1981 (Indiana University Cyclotron Facility)*, Ref. 2, p. 65.
[32]G. Jones, Nucl. Phys. **A416**, 157c (1984).
[33]D. V. Bugg, Nucl. Phys. **A416**, 227c (1984).
[34]Z. J. Cao and W. Y. P. Hwang, Phys. Rev. C **34**, 1785 (1986); Z. J. Cao, Ph.D. thesis, Indiana University, 1986.
[35]S. E. Vigdor, W. W. Jacobs, and E. Korkmaz, Phys. Rev. Lett. **58**, 840 (1987).
[36]E. Piasetzky *et al.*, Phys. Rev. Lett. **57**, 2135 (1986).
[37]S. H. Rokni, Ph.D. thesis, Utah State University, 1987; Los Alamos Meson Physics Facility Report LA-11004-T, 1987.
[38]B. D. Keister and L. S. Kisslinger, Nucl. Phys. **A412**, 301 (1984).
[39]M. J. Iqbal and G. E. Walker, Phys. Rev. C **32**, 557 (1985).
[40]K. Sakamoto, M. Hirata, A. Matsuyama, and K. Yazaki, Phys. Rev. C **31**, 1987 (1985).